16th World Conference on Earthquake, 16WCEE 2017

Santiago Chile, January 9th to 13th 2017

Paper N° 3604 (Abstract ID)

Registration Code: S-W1463208765

SEISMIC FRAGILITY ANALYSIS OF LIQUID STORAGE STEEL TANKS CONSIDERING SHELL BUCKLING AND ANCHOR FAILURE BY ADDED-MASS METHOD

N. Mirzadeh [(1)], E. Alavi [(2)], K. Kildashti [(3)]

[(1)] M. Sc., Senior Structural Engineer, Sazeh Consultants, email: mirzadeh.neda@gmail.com
[(2)] Ph.D., Structural Engineering Department, Sazeh Consultants, emails: e.alavi@sazeh.co.ir; e.alavi@iiees.ac.ir
[(3)] Ph.D., Postdoctoral Research Fellow, CIE, Western Sydney University, email: k.kildashti@westernsydney.edu.au

Abstract

Liquid storage tanks are vulnerable to a wide variety of failures under severe seismic excitation. Among all failure modes shell buckling and anchor bolt failures are the most critical forms of damage. Sometimes combination of different modes intensifies or accelerates liquid storage tank's damage. Although the effect of each different failure modes has been studied separately by a number of researchers, few studies may have considered combination of main failure modes concurrently. Hence, in this paper, a cylindrical steel tank has been selected in order to study multiple damages due to dynamic loadings on the tank. All anchor bolts and steel thin wall and reinforced concrete pedestal have been modeled counting material and geometric non-linearity. The methodology for finite element modeling of fluid-structure interaction has included applying the added-mass strategy, followed by performing the numerical analyses. A suite of ground motions has been selected and matched to the target spectrum. Afterwards, incremental dynamic analyses have been conducted to obtain fragility curve according to simultaneous modes of failure. The results have indicated that anchor bolt failures along with shell buckling significantly have contributed to more flexible behavior of the thin-walled steel tank and distribution of buckling to upper-middle part of tank which might increase seismic effects on the tank. Also, the design of steel tanks needs more considerations beyond current codes in major earthquake prone zones.

Keywords: Liquid storage tank, anchor bolt failures, thin-walled buckling, fragility analysis, incremental dynamic analysis

1. Introduction

Earthquake loads endanger liquid storage tanks due to formation of a wide variety of possible failure mechanisms as a result of fluid-structure interaction. Among all failure modes, shell bucking and anchor failures are major reasons of steel tanks' damage. A number of design codes such as ACI 318-14 [1], address comprehensive research on behavior of cast-in-place anchors subjected to lateral loading. The emphasis of the codes on behavior of different anchor shapes and types shows the importance of anchor bolts on behavior of the whole structure. To avoid unexpected failure of structures including steel tanks, it is necessary to carefully consider anchor failure in the design. Also because of small thickness of steel tanks, buckling of steel wall is a crucial parameter in design and analysis of this type of structure. These various failure modes of anchored steel tanks such as buckling modes (elephant's foot, diamond shape and secondary buckling) and anchor failures have been addressed by different researchers separately [2]-[5]. However, an integrated study to include combinations of both thin wall buckling and anchor bolt failures simultaneously is quite few.

Assessment of structural performance under severe ground motions is required a practical index. One applicable criterion to assess the performance of steel storage tank is fragility curve. This criterion was used by O'Rourke & So [5] and Salzano *et.al* [6] in past studies although they did not apply fragility curve for multiple measures. In the present work, fragility curves due to multiple actions of buckling and anchor bolt failures have been achieved by means of incremental time-history analyses performed on a 3D model of a case study of anchored steel tank with a height-to-diameter ratio (H/D = 0.8). It is worthwhile to note that for capturing more accurate behavior of the steel tank, material and geometric nonlinearity of both steel and concrete have been included. The approach to model fluid-structure interaction of the studied steel tank has been added-mass method [7].

The general purpose finite element software ABAQUS [8] has been applied for nonlinear dynamic analyses. A set of seven multi-directional recorded accelerograms have been selected from PEER/NGA database [9] and spectrally matched to the site-specific target spectrum. Afterwards incremental dynamic analyses (IDA's) have been performed, and their results have been assessed to find relationships between proper intensity measures (IM's) and engineering demand parameters (EDP's) [10].

2. Modelling overview

Due to large capacity, main performance of cylindrical tanks is storing a variety of liquids, such as water, petroleum, chemicals, and liquefied natural gas. Therefore, satisfactory performance of tanks during strong ground excitation is critical for modern facilities. Several investigations have shown tanks that were inadequately designed or detailed have suffered extensive damage during past earthquakes. Main earthquake damage to steel storage tanks include steel thin wall buckling and anchor failures (Fig. 1). Although in some cases base shear overcome friction causing the tanks to slide, due to heavy weight of tanks, these cases are quite rare. Also uneven settlement of foundations causes some problems that need more soil investigation and subgrade modeling in probable cases. All these damages reveal the necessity of accurate tank's seismic modeling before earthquake happens in actual site.

An integrated analytical model is required to be consisting of geometric and material nonlinearity characteristics as well as hydrodynamics effects of liquids in rigid tanks. ABAQUS is efficient software which is able to accurately model steel thin wall anchor bolts, concrete pedestal and liquid-structure interaction simultaneously.

A broad tank with H/D=0.8 has been investigated in the current study, the geometric features of the tank have been shown in Fig. 2. In particular, filling level and geometries have been illustrated in the figure. The tank has been assumed without a roof structure. Because full base anchorage has been considered, the model has been clamped by means of 24 anchor bolts of M56 embedded in 2.8m height and 0.6m thick concrete circular pedestal in which material characteristics of different components will be reported in the following sections. For the tank structural proportioning, and anchor bolts sizing, API-2008 [11] and ASCE7-10 [12] have been used. Table 1 indicates information and data have been assumed to calculate earthquake loads.

(a) (b)

Fig. 1 – (a) Sloshing damage to upper shell of tank (courtesy of University of California at Berkeley); (b) Anchor elongation in 2001 (Nisqually Earthquake)

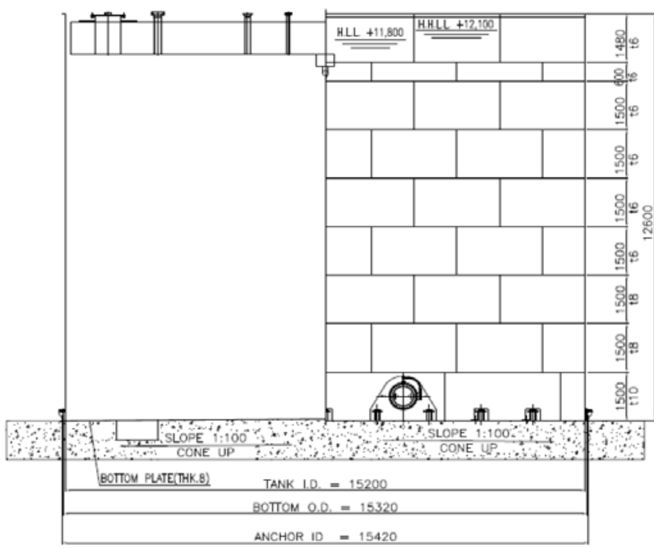

Fig. 2. Geometric features of the case study tank

2.1 Steel thin wall modeling

Combination of axial compression, global bending, internal and external pressure and cavitation in cylindrical tanks in the event of earthquake leads to different types of buckling. These types of buckling and post-buckling behavior are extremely dependent on the thickness of thin wall. Internal pressure and amplitude of imperfection in the shell cause the axial membrane stress that induces buckling in a shell. The final deformation of a tank is a function of internal pressure and axial compression force as well as a tank's wall thickness. To avoid premature buckling, some codes advice designers to select adequate thickness based on their recommendation [13], [14]. They provide some formulas to calculate so called "elephant's foot buckling" and "diamond-shape buckling". However, more sophisticated forms of buckling as a result of hydrodynamic pressure and self-weight of structure can be captured by finite-element analysis. In this study different types of buckling can be calculated by defining elastic-plastic behavior for steel material of the tank.

The four node doubly curved thin shell elements with quadrilateral linear geometric order and reduced integration finite membrane strain formulation (S4R) have been utilized to model thin-walled tank structure, in which in-plane and out-of-plane bending can be modeled simultaneously (Fig. 3(a)). Five integration points through the thickness of a homogenous shell with Simpson's rule have been used herein. The tank wall material is steel St37 with kinematic hardening constitutive behavior, in which mechanical properties are defined as: yield stress f_y=240 MPa, ultimate strength f_u=360 MPa, elastic modulus E=205 GPa and post-yielding modulus E_t=1.8 GPa.

Table 1 – Required parameters to calculate tank's earthquake

Parameter	**Value**	**Unit**
SUG : Seismic Use Group App. E (E.3.1) API	III	-
I : Importance Factor Coefficient set by Seismic Use Group App. E(Table E-5) API	1.5	-
R_{wi} : Force Reduction Factor for the Impulsive Mode App. E API	4	-
F_a : Acceleration-based site coefficient (at 0.2 sec period) App. E API	1.1	-
Q : Scaling factor from the MCE to the design level spectral accelerations (2/3 for ASCE 7-10 [12])	0.67	-
S_0 : Mapped, maximum considered earthquake, 5% damped, spectral response acceleration parameter at a period of zero seconds (peak ground acceleration for a rigid structure) (ASCE7-10)	0.45	%g
W_s : Total Weight of Tank Shell and Appurtenances	371	kN
W_r : Total Weight of Fixed Tank Roof Including Framing, Knuckles, any Permanent Attachments (10% for Accessories) and 10% of the Roof Design Snow load	450	kN
W_f : Weight of the Tank Bottom	113	kN
W_i : Effective Impulsive Portion of the Liquid Weight = [1 - 0.218 D / H] W_p	16,530	kN
W_p : Total Weight of Tank Content Based on Product Specific Gravity	22,429	kN

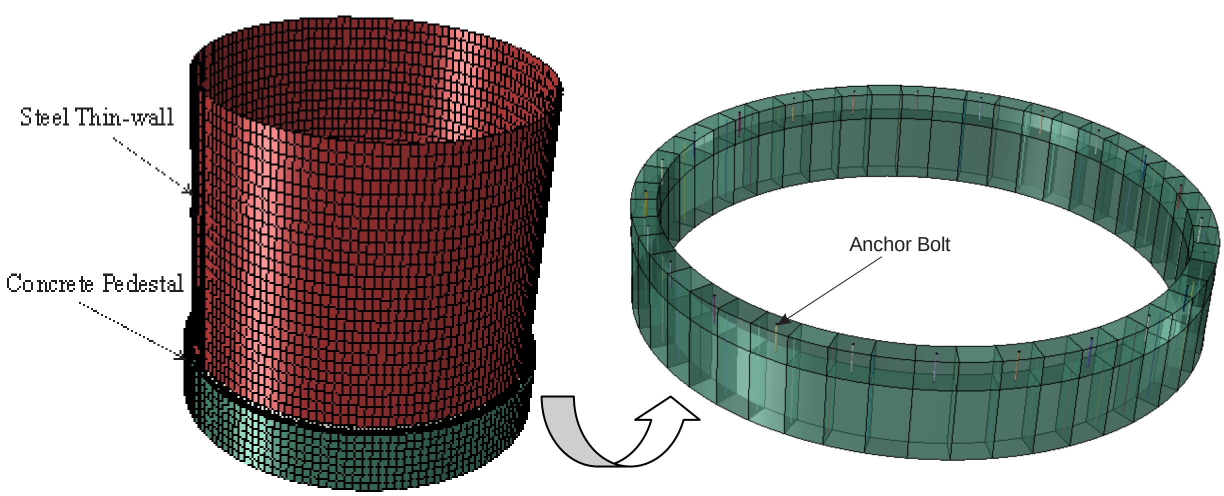

(a) (b)

Fig. 3– (a) Modeling in ABAQUS software (b) Anchor bolt modeling in ABAQUS software

2.2 Concrete pedestal modeling

Since anchor bolts are embedded in concrete ring pedestal, one main key point in determining the response of anchors and consequently the whole structure lies in the ability of the numerical models to accurately describe the concrete material nonlinearities. The eight node linear brick elements with reduced integration formulation (C3D8R) have been used to model concrete pedestal (Fig. 3(a)). The concrete constitutive behavior has been employed based on damaged plasticity model to represent the inelastic behavior of concrete [8]. By default, the yield function can be modeled for different evolution of strength under tension and compression and flow potential can be considered for the Drucker-Prager hyperbolic function. Fig. 4 illustrates the mechanical response of concrete under cyclic loading, in which w_c and w_t are the compressive and tensile stiffness recovery factor, respectively. Cylindrical concrete specific strength has been considered equal to 25 MPa and Mander *et.al* [15] formulation for unconfined concrete has been adopted to represent concrete monotonic behavior.

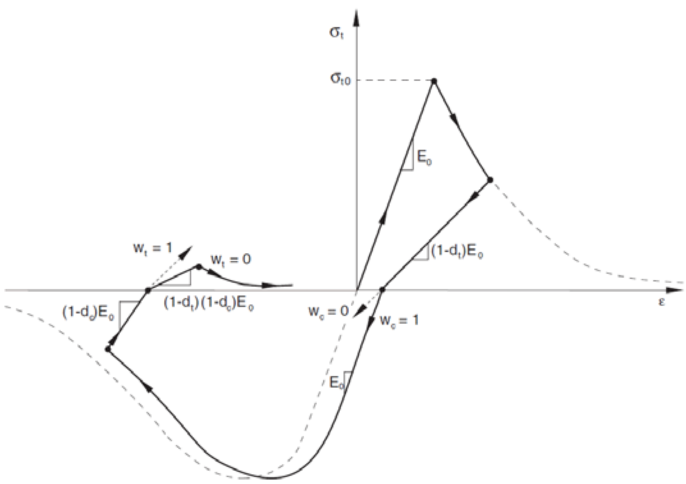

Fig. 4 – Uniaxial load cycle assuming default values for the stiffness recovery factors; d_t , d_c are compressive and tensile damage variables, respectively, E_0 is elastic modulus

2.3 Anchor bolt modeling

Steel anchorage are connection of steel superstructures to concrete pedestals or foundations. Since the whole loads of steel structure are supposed to be transferred to foundation by means of anchors, they play fundamental role in behavior of structure. Anchors can be either cast in concrete or post-installed into a hardened concrete member. Cast-in anchors include headed bolts, hooked bolts (J or L bolt), and headed studs. Performance of anchor bolts under lateral loading has been previously examined by analytical and experimental investigation. ACI 318-14 [1] provides design requirements for anchors in concrete used to transfer structural loads by means of tension, shear, or a combination of tension and shear. Since the seismic shear load is mainly resisted by the friction reverse force between the tank bottom and the sub-grade, only the tensile load due to the overturning moment is deemed to be supported by the anchors. Material, shapes and size of anchor bolts are critical to determine the behavior of them. In this study all anchors have been modeled based on exact length and material property. The anchor material has been selected as the steel Gr. B7 A193 ASTM with kinematic hardening constitutive behavior in which; the yield strength is F_y = 485 MPa, the ultimate strength is F_u = 620 MPa, and the effective cross sectional area is 18.63 cm^2. Fig. 3(b) shows embedded anchor bolts modeling in the concrete pedestal.

2.4 Liquid-structure interaction

The way that a tank and its content is modeled contribute to overall response of structure. During recent decades, researchers have proposed different methods to model impulsive and convective effects of liquid on tank's body

[16]-[18]. Some convenient methods just consider two or more lumped-mass and equivalent springs for tank-liquid simulation. More accurate and sophisticated approaches use added-mass distribution [2], [7]. Added masses are attributed to pressure distribution of rigid tanks and connected to the tank body by means of some links. In this study the added mass method has been used for modeling of cylindrical liquid storage tanks. In fact, added mass is produced as a consequence of pressure distribution and can be linked in shell nodes by pined rigid links (Fig. 5). Deriving from pressure distribution, added mass inertia is required to be normal to shell surface. In ABAQUS normal direction of shell nodes has been constrained to the motion of nodal masses. The restraints of linking elements have been tangentially and vertically restricted but they have been allowed to radially move. The impulsive pressure distribution has been obtained from the horizontal rigid body motion of a rigid tank-liquid system and can be expressed in a cylindrical reference system:

$$p_i(\eta,\theta,t) = c_i(\eta).\ddot{x}_g(t).\rho.R.\cos(\theta) \tag{1}$$

Where, (η) indicates the coordinate along the axis of the cylinder, θ is the circumferential position, t is the general time $\ddot{x}_g(t)$ is the ground acceleration time history, ρ is the water density, and the function $c_i(\eta)$ describes the pressure distribution along the tank's height[2]. The lumped mass at each node of the mesh is computed by multiplying the pressure acting on the tank walls (Eq. (1)) by the tributary area of the node and dividing by the reference ground acceleration $a_n = \ddot{x}_g(t).\cos(\theta)$. Therefore, for the general interior node, the expression of the lumped mass is given by equation (2).

$$m_i = \frac{p_i E_{size}^2}{a_n} = c_i(\eta).\rho.R.E_{size}^2 \tag{2}$$

Where, E_{size} is the mesh area of the rectangular finite elements.

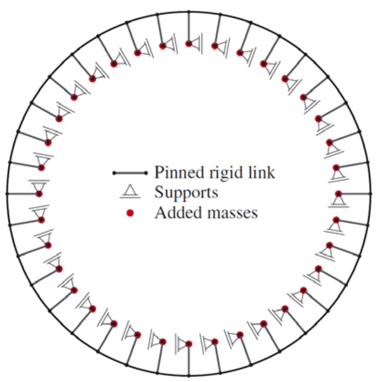

Fig. 5 – Representation of added mass model [2], [7]

3. Ground motion selection for fragility analysis

For the fragility analysis, 7 pairs of ground motion records have been selected from a subset of PEER/NGA database [9] (Table 2). The selection procedure has been adopted to obtain the best pairs of records satisfying seismic hazard condition, and site condition. The spectral-matching procedure has been utilized to adjust frequency content of accelerograms within predefined limits of a specified target spectrum. In particular, the 5% damped elastic target spectrum with 475 years return period has been calculated in accordance with recommendations of ASCE7-10 [12]. With the aim of spectral compatibility, the average of the 5% damped spectrum of all acceleration time histories has been approximately matched over period range 0.2T to 1.5T, where T is the fundamental period of vibration [12] (Fig. 6).

Table 2 – The 7 spectral-matched accelerograms used for fragility analysis

Record Seq. No.	Event	Year	Station	Magnitude (M_w)	Mechanism	R_{rup} (km)
RSN80	San Fernando, USA	1971	Old Seismo Lab	6.6	Reverse	21.5
RSN284	Irpinia, Italy	1980	Auletta	6.9	Normal	9.55
RSN675	Whittier Narrows, USA	1987	Pasadena-CIT Kresge Lab.	6.0	Reverse Oblique	18.12
RSN765	Loma Prieta, USA	1989	Gilroy Array#1	6.9	Reverse Oblique	9.64
RSN1011	Northridge, USA	1994	Wonderland Ave	6.7	Reverse	20.29
RSN1050	Northridge, USA	1994	Pacoima Dam (downstr)	6.7	Reverse	7.0
RSN2111	Denali, Alaska	2002	R109 (temp)	7.9	Strike slip	43.0

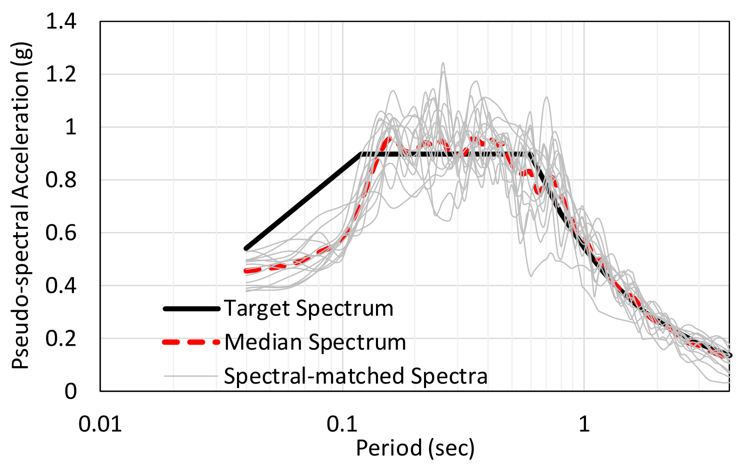

Fig. 6 – Response spectra of the 7 pairs of selected accelerograms and matching with the target spectrum

4. Seismic fragility analysis

Seismic fragility analyses provide the probability of occurrence for EDP's as a function of IM's. IM is a parameter defining the severity of ground motions on structures. Different IM's have been commonly introduced in literature including; the peak ground acceleration (PGA), the peak ground velocity (PGV), the peak ground displacement (PGD), and single or multiple pseudo spectral acceleration (PSA). The EDP's in the current paper have been mainly influenced by anchor bolt failure and elastic-plastic buckling. Different IDA's of the case study tank have been conducted and critical IM's have been obtained for which there has been a sudden jump in the EDP's due to slight increase in IM's. IDA's have been performed for multi-directional ground motions (in orthogonal directions). To obtain the most representative EDP's in the structure, four grids of points have been considered in those portions of the structure where the maximum deformations due to plasticization and buckling have been expected, and the critical node has been assumed to be the one that have developed the smallest IM (Fig. 7).

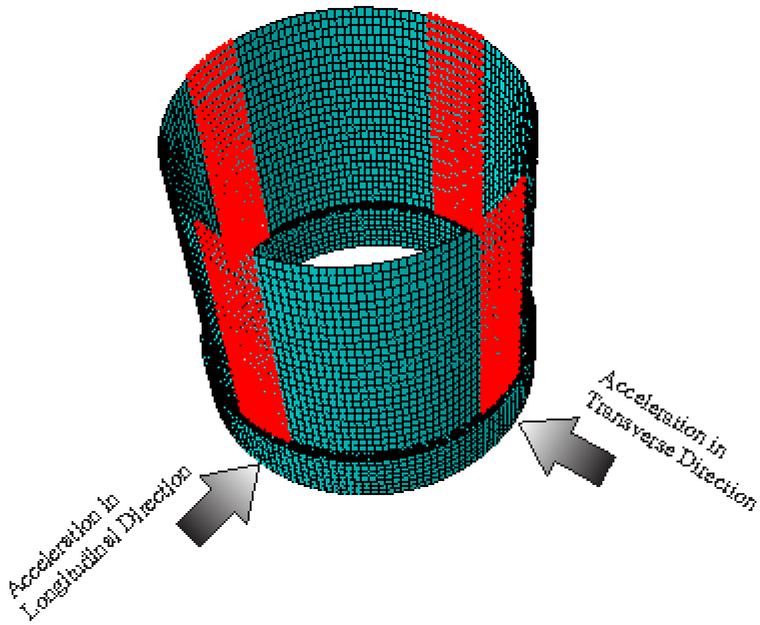

Fig. 7 – Four grids of points for which critical nodes need to be obtained

As can be observed in Fig. 8, displacement time histories for a critical node in the ABAQUS model based on transient analyses have been illustrated. Evidently, sudden jump in the values of displacement by increasing of PGA from 0.82g to 1.03g has indicated the incipient dynamic instability due to the combination of thin wall buckling and anchor bolt plasticization. Fig. 9 shows the deformed shape of the tank walls at the onset of local buckling.

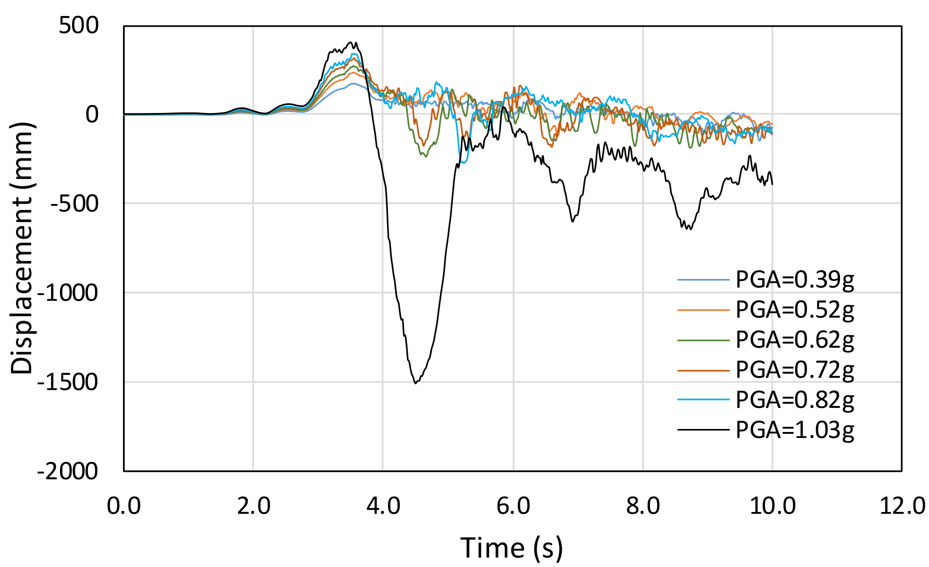

Fig. 8 – Time histories of a nodal displacement for increasing PGA values due to RSN765

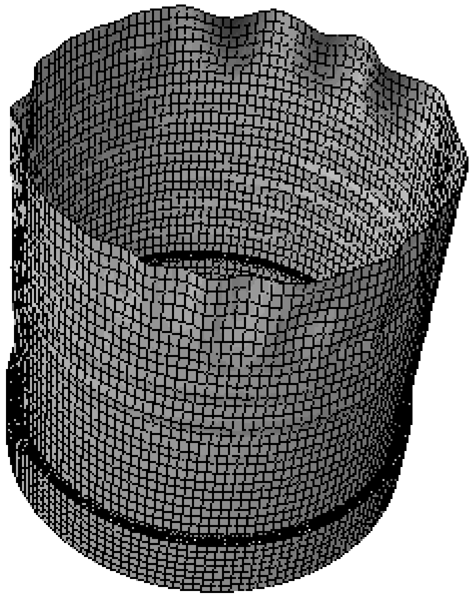

Fig. 9 – Deformed shape of the tank at the onset of local buckling

4.1 Fragility curve

The probability of failure (P_f) predominantly defines a cumulative density function for the random variable (critical IM), which has been described by critical PGA herein. Hence, it can be defined by the following relationship:

$$P_f = P(IM_{cr} \leq im) \tag{1}$$

As recommended in the literature, lognormal distribution is commonly used for the IM. Therefore, cumulative density function can be obtained by knowing the mean and standard deviation. In Fig. 10 (a) results of IDA curves for different time history analyses have been adopted to obtain critical IM. The fragility curve along with IDA data points have been illustrated in Fig. 10 (b). As can be observed, there has been a good agreement between analytical curve and IDA data points, as a result, the lognormal distribution model has been appropriate to obtain fragility curve of liquid-storage tanks.

According to fragility analysis, the structural vulnerability for 50% probability of occurrence has been assessed and the value of IM_{cr} has been obtained equal to 0.54g. Since the value of peak ground acceleration has been 0.45g (Table 1), the margin of safety against onset of failure can be easily calculated as a ratio of 0.54g/0.45g=1.2.

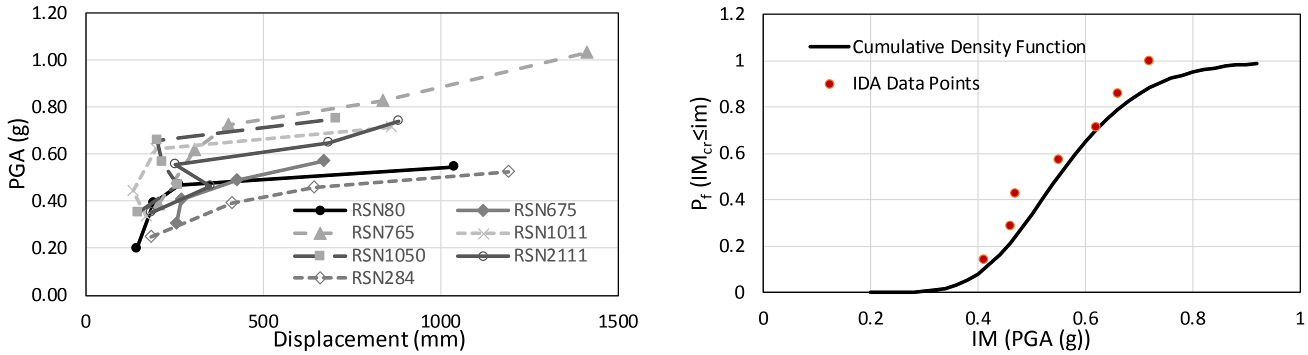

(a) (b)

Fig. 10 – (a) IDA curves for different ground motion records (b) Lognormal fragility curve for combination of elastic-plastic thin wall buckling and anchor bolts failure

5. Conclusion

In the present research, a liquid storage tank's failure modes were studied. To investigate more accurate combination of failure modes, such as anchor failures and steel buckling, all anchor bolts, steel thin wall and reinforced concrete pedestal were modeled considering material and geometric nonlinearities. The results can be categorized as the followings;

- Modelling of all components and material characteristics of storage tank allow the structure to behave more flexibly. As a result, the dominant failure mode which occurred at the upper-middle part of shell could be presented. But by modeling a tank as a fixed based structure, it was expected that some critical buckling modes happened at the bottom of tank due to stress concentration.
- Elastic-plastic behavior of anchor bolts and concrete were able to damp earthquake energy as it happened in reality; so, margin of safety could be estimated more accurately.
- Considering the results of fragility analysis, design of steel storage tanks in accordance with current standard requirement does not necessarily provide adequate safeguard against premature failure for all kinds of earthquake prone regions.

6. References

[1] ACI318-14. (2014): Building code requirements for structural concrete and commentary. Farmington Hills, MI: American Concrete Institute Committee 318.

[2] Burati N, Tavano M (2014): Dynamic buckling and seismic fragility of anchored steel tanks by the added mass method. *Earthquake Engineering & Structural Dynamics*, **43** (1), 1-21.

[3] Brown KJ, Rugar P, Davis C, Rulla T (1995): Seismic performance of Los Angeles water tanks. Fourth U.S. Conference on Lifeline Earthquake Engineering, San Francisco, USA. 668-675.

[4] Haroun MA, (1983): Behavior of unanchored oil storage tanks: Imperial Valley Earthquake. *Journal of Technical Topics in Civil Engineering*, **109** (1), 23-40.

[5] O'Rourke MJ, So P (2000): Seismic fragility curves for on-grade steel tanks. *Earthquake Spectra*, **16**(4), 801-815.

[6] Salzano E, Iervolino I, Fabbrocino E (2003): Seismic risk of atmospheric storage tanks in the framework of quantitative risk analysis. *Journal of Loss Prevention in the Process Industries*, **16**(5), 403-409.

[7] Virella JC, Godoy LA, Suárez LE (2006): Dynamic buckling of anchored steel tanks subjected to horizontal earthquake excitation. *Journal of Constructional Steel Research*, 62, 521-531.

[8] ABAQUS. (2005): User's manual. Providence: Hibbit and Karlson and Sorensen.

[9] PEER NGA-West2 Data Base. (2014): Pacific earthquake engineering research (PEER). Berkeley: University of California. Retrieved from http://ngawest2.berkeley.edu/

[10] Vamvatsikos D, Cornell CA (2002): Incremental dynamic analysis. *Earthquake Engineering & Structural Dynamics*, **31** (3), 491-514.

[11] API (2008): Welded Tanks for Oil Storage, API Publishing Services, 1220 L Street, N W, Washington, D.C. 20005.

[12] ASCE7-10 (2010): Minimum design loads for buildings and other structures. Reston, VA: American Society of Civil Engineering (ASCE).

[13] European Convention for Constructional Steelwork (ECCS) (1988): Buckling of Steel Shells - European Recommendations (4th Edition), ECCS: Brussels, Belgium.

[14] Tavano M (2012): Seismic response of tank-fluid systems: state of the art review and dynamic buckling analysis of a steel tank with the added mass method, in Department of Civil, Environmental and Materials Engineering, University of Bologna.

[15] Mander, JB, Priestley MJN, Park R (1984): Theoretical Stress-Strain Model for Confined Concrete. *Journal of Structural Engineering ASCE* **114**: 1804-1826.

[16] Fischer FD, Rammerstorfer FG (1999): A refined analysis of sloshing effects in seismically excited tanks. *International Journal of Pressure Vessels and Piping*, **76**(10), 693–709.

[17] Zienkiewicz OC, Taylor RL, Nithiarasu P (2005): The finite element method for fluid dynamics. 6th Edition, Amsterdam; London: Elsevier Butterworth-Heinemann.

[18] Kim MK, Lim YM, Cho SY, Cho KH, Lee KW (2002): Seismic analysis of base-isolated liquid storage tanks using the BE–FE–BE coupling technique. *Soil Dynamics and Earthquake Engineering*, **22** (9-12):1151-1158.